

# Improve low-temperature selective catalytic reduction of NO<sub>x</sub> with NH<sub>3</sub> by ozone injection

Meiyi Liu<sup>1,3</sup>, Jie Li<sup>1,2,3,\*</sup>, Zhengyan Liu<sup>1,3</sup>, Yonghe Zhao<sup>1,3</sup>, Nan Jiang<sup>1,2,3</sup>, Yan Wu<sup>1,2,3</sup>

<sup>1</sup> Key Laboratory of Industrial Ecology and Environmental Engineering, MOE, Dalian University of Technology, Dalian 116024, China

<sup>2</sup> School of Electrical Engineering, Dalian University of Technology, Dalian 116024, China

<sup>3</sup> School of Environmental Science & Technology, Dalian University of Technology, Dalian 116024, China

\* Corresponding author: [lijie@dlut.edu.cn](mailto:lijie@dlut.edu.cn) (Jie Li)

Received: 15 January 2020

Revised: 16 March 2020

Accepted: 24 March 2020

Published online: 28 March 2020

## Abstract

Low-temperature selective catalytic reduction (SCR) is an important technology for the abatement of the nitrogen oxides (NO<sub>x</sub>) from stationary sources. The research of fast SCR process has attracted many attentions. In this study, the ozone generated by dielectric barrier discharge oxidized NO to achieve the fast SCR process. We found that the combination of O<sub>3</sub> and SCR can effectively reduce NO<sub>x</sub> emissions at low temperature ( $\leq 250$  °C). At 250 °C, the removal efficiency of NO<sub>x</sub> in O<sub>3</sub>-NH<sub>3</sub>-SCR process (molar ratio of O<sub>3</sub>/NO = 0.5) reached 88.3%, while the standard SCR was only 56.8%. Furthermore, the effects of H<sub>2</sub>O and SO<sub>2</sub> on NO<sub>x</sub> removal using ozone assisted SCR system were also explored.

**Keywords:** Dielectric-barrier discharge, O<sub>3</sub>, CeO<sub>2</sub> catalyst, SCR, De-NO<sub>x</sub>.

## 1. Introduction

According to the US Environmental Protection Agency (EPA), the sources of nitrogen oxides [NO<sub>x</sub> (x = 1, 2)] mainly include the combustion of electric and thermal fuel, the discharge of transportation processes and industrial production processes [1]. Usually, more than 90% of the NO<sub>x</sub> in the flue gas is NO, which can pose serious environmental problems such as acid rain, photochemical smog, ozone depletion, the greenhouse effect, etc. [2]. Selective catalytic reduction (SCR) technology is widely used in coal-fired flue gas for the removal of nitrogen oxides. The typical standard SCR process ( $4\text{NO} + 4\text{NH}_3 + \text{O}_2 \rightarrow 6\text{H}_2\text{O} + 4\text{N}_2$ ) uses NH<sub>3</sub> as a reducing agent to convert NO<sub>x</sub> to nitrogen and water in combination with the catalyst [3–5]. However, the problems of narrow operating temperature window of catalysts and low catalytic activity below 250 °C have been widely reported [6, 7]. One way to improve efficiency is to make the ratio of NO to NO<sub>2</sub> about 1:1, which is called fast SCR process ( $4\text{NH}_3 + 2\text{NO}_2 + 2\text{NO} \rightarrow 4\text{N}_2 + 6\text{H}_2\text{O}$ ) [8–10]. The fast SCR process can be achieved by converting 50% NO to NO<sub>2</sub> before contacting the catalyst [11, 12]. Therefore, the oxidation of NO to NO<sub>2</sub> is a key factor and rate determining step for entire fast SCR reaction. In recent years, fast SCR has received much attention due to its potential in low temperature SCR process [13]. The research and development of fast SCR technology aim to improve the SCR denitration efficiency at low temperature and reduce the amount of catalysts [14]. At present, pre-oxidation techniques are effective method to realize the fast SCR process, which include non-thermal plasma oxidation [15], electron beam flue gas treatment [16], photocatalytic oxidation absorption [17] and direct oxidation [18–21]. The NO<sub>x</sub> oxidation method by ozone injection has several advantages compared with other techniques, for examples, the ozone injection method keeps the plasma discharge clean compared to the direct oxidation in an oxygen-containing flue gas using an oxidation reactor, which also has a stronger oxidation selectivity for NO [22, 23]. Despite of these positive points, the low-temperature oxidation technology is still relatively expensive and requires further optimization for the overall process. The main methods for generating ozone include ultraviolet irradiation, electrolytic method, radiochemical method, and dielectric barrier discharge. Dielectric barrier discharge method dissociates oxygen

molecules by high-energy electrons generated in a gas by a high-voltage electric field and polymerizes into ozone molecules by collision. This method has been widely used in industry due to its advantages such as relatively low energy consumption and large ozone output [24].

Vanadium-based catalysts have achieved great success only in the field of high-temperature SCR, and it is more important to develop new catalysts with low temperature and high activity. Some transition metals such as Mn, Ce, Cu, Fe are believed to exhibit higher activity during the selective catalytic reduction of NO with NH<sub>3</sub>. Luo *et al.* reported that the 5 wt%  $\gamma$ -MnO<sub>2</sub>/TiO<sub>2</sub> supported catalysts can achieve almost 100% NOx conversion at 200–300 °C in SCR experiment [25]. Jesús *et al.* used CuO/NiO monolithic catalysts to achieve a NOx conversion of about 90 % at 230 °C [26]. CeO<sub>2</sub> is a non-toxic and environment friendly transition oxide, due to its superior strong oxygen storage and release property via the redox cycle between Ce<sup>4+</sup> and Ce<sup>3+</sup>, which has been widely used for NOx removal [27]. Shan *et al.* reported that Ce–Ti based catalyst showed over 90% NOx conversion at a temperature of 450 °C under a GHSV of 20000 h<sup>-1</sup> [28]. Gao *et al.* found that Ce–Cu–Ti has the largest specific surface area and pore volume, and presents high activity of NO removal at the temperature range from 200 °C to 400 °C [29]. Li *et al.* prepared a novel Ce–Mo–Ox catalyst, which showed excellent activity and maintained NOx removal efficiency above 90% in the temperature range of 200–350 °C [30].

Although many studies have reported the method of NO pretreatment by ozone oxidation, few studies have reported the effect of ozone injection location on NO oxidation and NOx removal. Furthermore, the effects of H<sub>2</sub>O and SO<sub>2</sub> on NOx removal by O<sub>3</sub> assisted SCR flue gas are also rarely reported. In this paper, an experimental study was carried out to improve the efficiency of NOx removal at low temperature by ozone assisted SCR process. The effects of simulated flue temperature, O<sub>3</sub>/NO molar ratio, and residence time on NO oxidation efficiency were studied. Moreover, the effects of O<sub>3</sub>/NO molar ratio, O<sub>3</sub> injection location, H<sub>2</sub>O and SO<sub>2</sub> on the ozone assisted SCR process were also investigated.

## 2. Experimental system

### 2.1 Catalyst Preparation

CeO<sub>2</sub> catalyst was prepared by using cerium nitrate (Ce(NO<sub>3</sub>)<sub>3</sub>·6H<sub>2</sub>O) as precursor and oxalic acid (H<sub>2</sub>C<sub>2</sub>O<sub>4</sub>·2H<sub>2</sub>O) as precipitant. A certain amount of cerium nitrate was dissolved in the solution, then the excess oxalic acid was added to the solution under strong agitation and mixed evenly until the solution was completely precipitated. The sample was filtered and dried at 100 °C for 10 h, and successively calcined at 500 °C for 5h. The obtained catalyst was denoted as CeO<sub>2</sub>. The CeO<sub>2</sub> powder catalyst was pressed and crushed to 20–40 mesh before the activity tests.

### 2.2 Experimental setup

The schematic diagram of the experimental device is presented in Fig. 1. It consists of a simulated flue gas mixing unit, a temperature control device, an ozone generator, a SCR reactor and gas analysis devices. The simulated flue gas was from gas cylinders (N<sub>2</sub>, 99.99%; O<sub>2</sub>, 99.99%; NO, 5%, balanced with N<sub>2</sub>; SO<sub>2</sub>, 99.99%; NH<sub>3</sub>, 1.5%, balanced with Ar). The typical simulated flue gas composition was as follows: [NO] = [NH<sub>3</sub>] = 500 ppm, [O<sub>2</sub>] = 3 vol.%, [SO<sub>2</sub>] = 200 ppm (when used), and N<sub>2</sub> was the carrier gas. The total flow rate of the gas was maintained at 1.0 L·min<sup>-1</sup>. In order to determine the influences of operating temperature on each process, the mixing units and SCR reactor were placed in the tubular furnace. The simulated flue gas was mixed and heated to the target temperature in the mixing preheater, then the simulated gas was fed into the ozone oxidation system and the SCR reactor. The SCR reactor was made of a quartz tube (40 cm length × 16 mm i.d.) filled with CeO<sub>2</sub> catalyst. The Gas hourly specific velocity (GHSV) was calculated based on the residence time of the gas in the catalyst. The ozone generator structure used in the experiment was a coaxial cylindrical dielectric barrier discharge reactor. A stainless steel rod with a diameter of 4 mm and a length of 370 mm was used as a high-voltage electrode, a ceramic tube with a length of 250 mm and an outer diameter of 10 mm was used as a dielectric. The ceramic tube was provided with a plexiglass tube with an outer diameter of 30 mm and a diameter of 150 mm, and circulating cooling water between them served as a ground electrode. Power supply used in this experiment was high frequency AC power supply (CTP-2000K). Water vapor was introduced by inletting simulated gas through temperature-controlled bubble system containing deionized

water and the water content was varied from 0 vol.% to 6 vol.%. A flue gas analyzer (Testo 350) was used to monitor the concentration of NO and NO<sub>2</sub> in the simulated flue gas online. Ozone was monitored online by an ozone analyzer (2B Technologies), SO<sub>2</sub> and the composition of gas phase were determined by Fourier transform infrared spectroscopy (FTIR, Nicolet 6700), and flue gas humidity was measured using a thermo-hygrometer (HP21, Rotronic).

The NO oxidation efficiency and the NO<sub>x</sub> removal efficiency were calculated according to the following equation:

$$\text{NO}_{\text{conversion}}(\%) = \frac{[\text{NO}]_{\text{in}} - [\text{NO}]_{\text{out}}}{[\text{NO}]_{\text{in}}} \times 100\% \quad (1)$$

$$\text{NO}_{\text{x removal}}(\%) = \frac{[\text{NO}_{\text{x}}]_{\text{in}} - [\text{NO}_{\text{x}}]_{\text{out}}}{[\text{NO}_{\text{x}}]_{\text{in}}} \times 100\% \quad (2)$$

Where [NO]<sub>in</sub>, [NO<sub>x</sub>]<sub>in</sub> and [NO]<sub>out</sub>, [NO<sub>x</sub>]<sub>out</sub> represent the concentrations of NO and NO<sub>x</sub> in the inlet and outlet gases respectively.

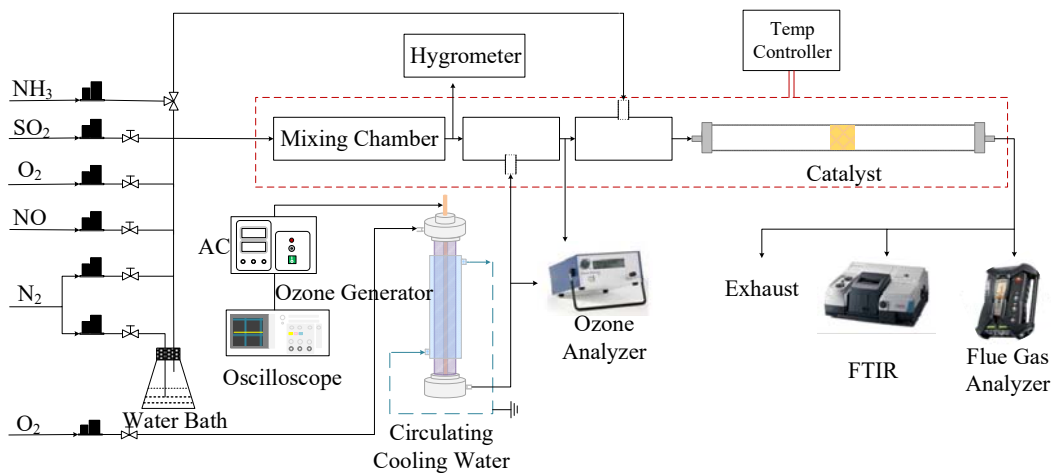


Fig.1. Schematic of the experimental setup for O<sub>3</sub> assisted SCR system.

### 3. Results and discussion

#### 3.1 The influence of NO oxidation

Fig. 2 shows the ozone production and O<sub>3</sub>/NO molar ratio as a function of discharge voltage. As shown in Fig. 2, the ozone concentration increased with the discharge voltage increased, while the discharge voltage increased from 5.6 kV to 6.4 kV with the O<sub>3</sub>/NO molar ratio increased from 0.2 to 0.8. These results indicated that the enhancement of O<sub>3</sub> concentration can effectively oxidize NO. In this experiment, the initial simulated flue gas only contained NO, so the oxidation of NO was the key to achieve fast SCR and efficient NO<sub>x</sub> removal. Fig. 3 shows the effect of molar ratio of O<sub>3</sub>/NO on the oxidation efficiency of NO. As the residence time of the simulated flue gas in the heating furnace increased from 2 s to 6 s, the oxidation efficiency of NO did not change significantly. There was a certain deviation of NO oxidation efficiency within 6 s, which might be due to fluctuations in simulated smoke concentration or ozone generation. The oxidation products of NO at different O<sub>3</sub>/NO molar ratios were analyzed by FTIR. As shown in Fig. 4, with the O<sub>3</sub>/NO molar ratio ( $\leq 0.8$ ) increased, the peak intensity at 1900 cm<sup>-1</sup> declined gradually, while the peak intensity at 1600 cm<sup>-1</sup> and 2919 cm<sup>-1</sup> increased. Correspondingly, the characteristic peak of NO gradually disappeared, while the intensity of NO<sub>2</sub> characteristic gradually improved. Only NO<sub>2</sub> was detected in the oxidation products, and no characteristic peaks of NO<sub>3</sub> and N<sub>2</sub>O<sub>5</sub> were observed in FTIR. These results suggested that the increase of the molar ratio of O<sub>3</sub>/NO ( $\leq 0.8$ ) can effectively oxidize NO to NO<sub>2</sub>. In addition, a series of kinetic model parameters during NO oxidation in this experiment were obtained from data in the National Institute of Standards and Technology (NIST) database, as shown in formulas (3)–(5).

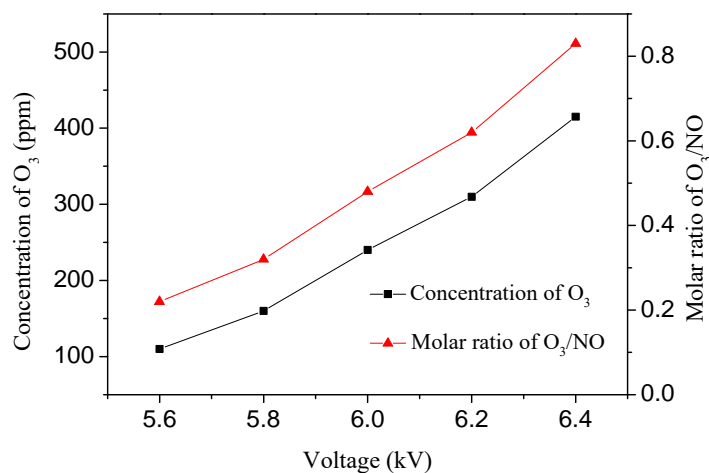


Fig. 2. O<sub>3</sub> concentration at different voltages. Conditions: [NO]<sub>in</sub> = 500 ppm, O<sub>2</sub> flow rate = 10 mL·min<sup>-1</sup>, and flue gas flow rate = 1.0 L·min<sup>-1</sup>.

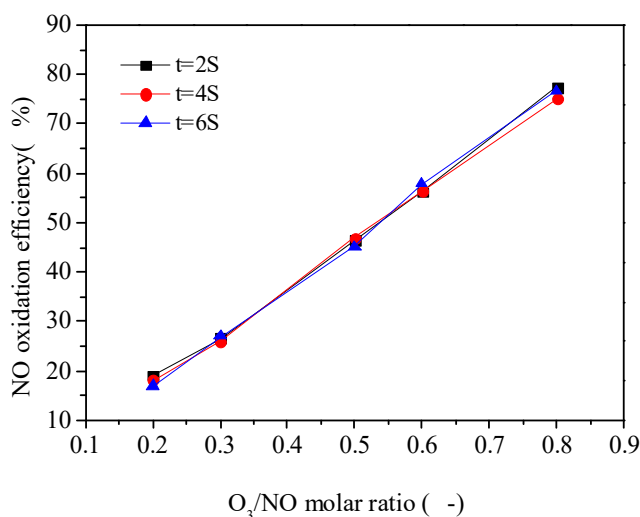
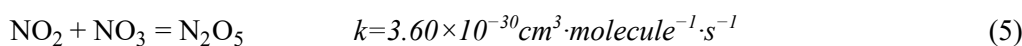
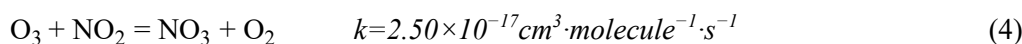
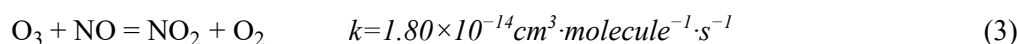


Fig. 3. Effect of the molar ratio of O<sub>3</sub>/NO on NO oxidation efficiency. Conditions: [NO]<sub>in</sub> = 500 ppm, flue gas temperature = 150 °C, and flue gas flow rate = 1.0 L·min<sup>-1</sup>.



Considering the temperature range of standard SCR flue gas is usually within 400 °C, the effect of reaction temperature on NO oxidation efficiency by O<sub>3</sub> was investigated, as shown in Fig. 5, When the simulated flue gas temperature was 100 °C and the molar ratio of O<sub>3</sub>/NO was 0.5, the oxidation efficiency of NO was 45.36%. However, the oxidation efficiency of NO decreased significantly with the increase of reaction temperature. In particular, the oxidation efficiency of NO was only 3.55% at 400 °C. With the temperature of the flue gas raised, the self-decomposition rate of ozone accelerated, which led to the decrease of NO oxidation efficiency. Therefore, an appropriate temperature condition should be selected to reduce the loss of thermal decomposition of O<sub>3</sub> during NO oxidation process.

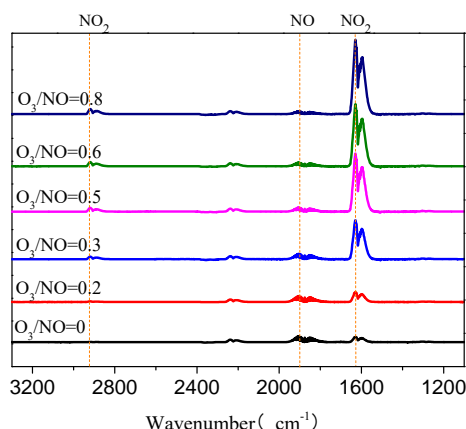


Fig. 4. Effect of the molar ratio of  $O_3/NO$  on NO oxidation products. Conditions:  $[NO]_{in} = 500$  ppm, flue gas temperature =  $150^\circ C$ , residence time = 2 s, and flue gas flow rate =  $1.0 L \cdot min^{-1}$ .

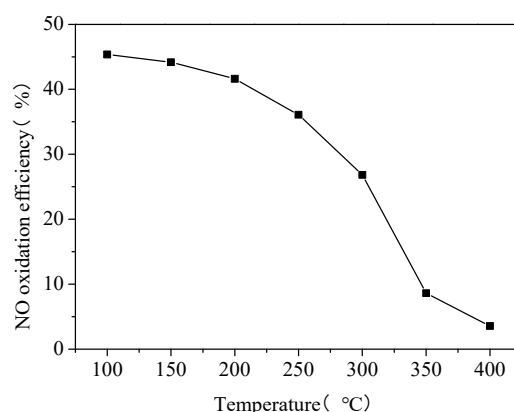


Fig. 5. Effect of gas temperature on NO oxidation efficiency by  $O_3$ . Conditions:  $[NO]_{in} = 500$  ppm,  $O_3$  concentration = 250 ppm, residence time = 2 s, and flue gas flow rate =  $1.0 L \cdot min^{-1}$ .

### 3.2 Effect of $O_3/NO$ molar ratio on the NOx removal

The effect of the molar ratio of  $O_3/NO$  on NOx removal efficiency in ozone assisted SCR system is investigated in Fig. 6. As the temperature raised from  $100^\circ C$  to  $350^\circ C$ , the NOx removal efficiency increased significantly from 8.8% to 71.8%. However, the NOx removal efficiency started to decline rapidly in the SCR process, when the temperature reached  $400^\circ C$ . This result can be attributed to the activation energy required for the removal of NOx by the standard SCR process was higher. Since the activation temperature of the catalyst did not reach at a low temperature, the efficiency of NOx removal was low. As the temperature of the flue gas gradually increased, the catalytic activity was excited, which enhanced the NOx removal efficiency under the presence of  $NH_3$  in formula 6. When the temperature exceeded  $400^\circ C$ , the NOx removal efficiency significantly decreased, which can be attributed to the deactivation of catalyst due to the high temperatures. In addition, the NOx removal efficiency could markedly enhance with the injection of  $O_3$ , and that increased from 67.4% to 88.0% with the  $O_3/NO$  molar ratio increased from 0.2 to 0.5 at a temperature of  $250^\circ C$ . However, when the  $O_3/NO$  molar ratio further increased by 0.6, the NOx removal efficiency slightly decreased. This result indicated that the  $O_3/NO$  molar ratio of 0.5 might be the optimal value to realize the fast SCR process (Formula 7).



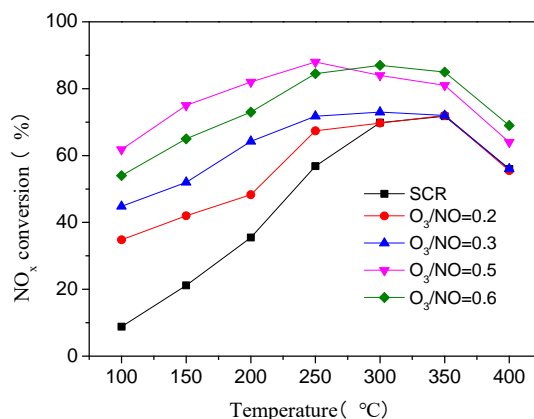


Fig. 6. Effect of O<sub>3</sub>/NO molar ratio on removal of NO<sub>x</sub> by O<sub>3</sub>-NH<sub>3</sub>-SCR process. Conditions: [NO]<sub>in</sub> = [NH<sub>3</sub>] = 500 ppm, [O<sub>2</sub>] concentration = 3%, residence time = 2 s, and flue gas flow rate = 1.0 L·min<sup>-1</sup>, GHSV = 25000 h<sup>-1</sup>.

### 3.3 Effect of O<sub>3</sub> assisted NH<sub>3</sub>-SCR on NO<sub>x</sub> removal

Fig. 7 shows the effect of two injection locations of O<sub>3</sub> upstream and downstream (denoted as O<sub>3</sub>-NH<sub>3</sub>-SCR and NH<sub>3</sub>-O<sub>3</sub>-SCR, respectively) NH<sub>3</sub> on NO<sub>x</sub> removal of flue gas in O<sub>3</sub> assisted SCR process. The result showed that the NH<sub>3</sub>-O<sub>3</sub>-SCR method and the O<sub>3</sub>-NH<sub>3</sub>-SCR method had a NO<sub>x</sub> removal efficiency of 82.0% and 88.3% at 250 °C, respectively, while the best removal efficiency of standard SCR at 350 °C was only 71.8%. It can be seen that, compared with the standard SCR process, the injection of O<sub>3</sub> can significantly enhance the NO<sub>x</sub> removal efficiency at the same temperature and the temperature of largest removal efficiency could be effectively decreased in O<sub>3</sub> assisted SCR process. Moreover, the NO<sub>x</sub> removal efficiency in O<sub>3</sub>-NH<sub>3</sub>-SCR system was larger than that in NH<sub>3</sub>-O<sub>3</sub>-SCR system. When the temperature exceeded 250 °C, both the NO<sub>x</sub> removal efficiency in O<sub>3</sub>-NH<sub>3</sub>-SCR and NH<sub>3</sub>-O<sub>3</sub>-SCR system began to decrease, which can be described to the O<sub>3</sub> rapid decomposition due to the high reaction temperature.

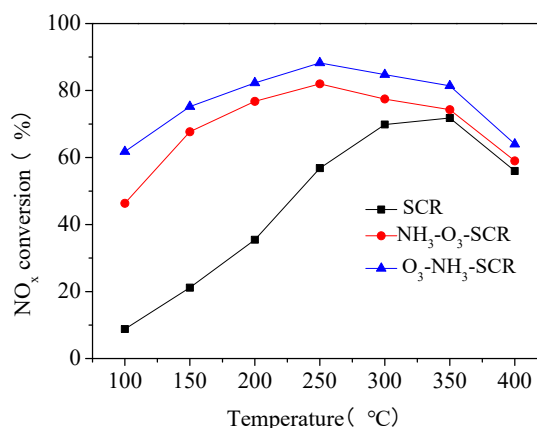


Fig. 7. Effect of O<sub>3</sub> injection position assisted SCR on NO<sub>x</sub> removal efficiency. Conditions: [NO]<sub>in</sub> = [NH<sub>3</sub>] = 500 ppm, O<sub>3</sub> concentration = 250 ppm, flue gas flow rate = 1.0 L·min<sup>-1</sup>, and GHSV = 25000 h<sup>-1</sup>.

In order to analyze the possible reasons for the difference in NO removal efficiency between the NH<sub>3</sub>-O<sub>3</sub>-SCR process and the O<sub>3</sub>-NH<sub>3</sub>-SCR process, the effect of NO oxidation efficiency by ozone and NH<sub>3</sub> injection locations in simulated flue gas was analyzed. As shown in Fig. 8, the NO oxidation effect of O<sub>3</sub>-NH<sub>3</sub> system was better than NH<sub>3</sub>-O<sub>3</sub> system in the range of the O<sub>3</sub>/NO molar ratio from 0.2 to 0.8. This result might be described to the oxidation reaction of ozone with ammonia consumed part of ozone, resulting in a decrease in the oxidation efficiency of NO in NH<sub>3</sub>-O<sub>3</sub> system (Formula 8) [31].



In order to verify the presence of ammonium nitrate, the  $\text{NO}_3^-$  content of the exhaust gas was measured. The method of collecting ammonium nitrate was to filter the gas online at the outlet during the reaction by using a micron-sized fiber gas particulate filter. Then, the filter was placed in excess water for sonication to sufficiently dissolve the ammonium nitrate adhering to the filter. The  $\text{NO}_3^-$  in the dissolved ammonium nitrate solution was finally determined by ion chromatography to determine the yield of ammonium nitrate. The yield of ammonium nitrate was  $2.2 \text{ mg h}^{-1}$  at simulated flue gas temperatures of  $150 \text{ }^\circ\text{C}$ . This study suggested that the NO oxidation efficiency in the  $\text{O}_3\text{-NH}_3$  system was better than that in the  $\text{NH}_3\text{-O}_3$  system. When ozone was injected into the simulated flue gas after ammonia, ozone could react with ammonia to produce ammonium nitrate. In this process, ammonia could compete with NO for ozone, which affected the production of  $\text{NO}_2$  and reduced the removal efficiency of  $\text{NO}_x$  in the fast SCR process.

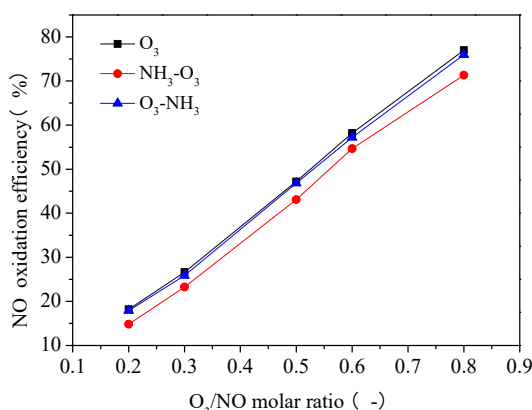


Fig. 8. Effect of  $\text{O}_3$  injection position on NO oxidation efficiency. Conditions:  $[\text{NO}]_{\text{in}} = [\text{NH}_3] = 500 \text{ ppm}$ ,  $\text{O}_2$  content = 3 vol.%, flue gas temperature =  $150 \text{ }^\circ\text{C}$ , residence time = 2 s, flue gas flow rate =  $1.0 \text{ L}\cdot\text{min}^{-1}$ .

### 3.4 Effect of $\text{H}_2\text{O}$ on the $\text{NO}_x$ removal

Fig. 9 shows the effect of  $\text{H}_2\text{O}$  on NO oxidation efficiency in simulated flue gas. The temperature of flue gas was kept at  $150 \text{ }^\circ\text{C}$ . The study showed that the addition of water vapor in the simulated flue gas reduced the oxidation efficiency of NO by  $\text{O}_3$ . When the content of water vapor in carrier gas was 0 vol.%, 2 vol.%, and 6 vol.%, the NO oxidation efficiency was 81.4%, 77.6%, and 70.0% at the  $\text{O}_3/\text{NO}$  molar ratio of 0.8, respectively. This result could be attributed to the loss of ozone in the experiment, because the ozone could react with  $\text{H}_2\text{O}$  and  $\text{H}_2\text{O}_2$  (Formula (9) and (10)) [32].

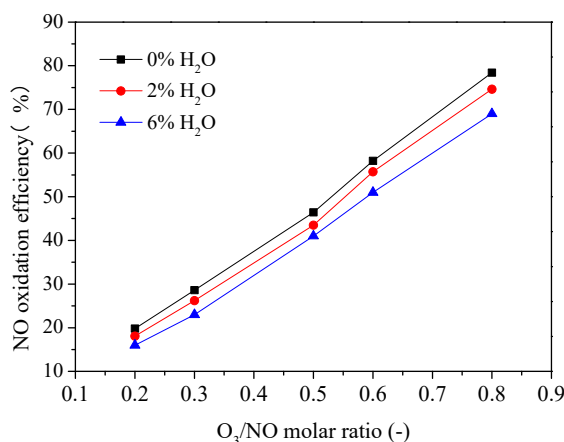
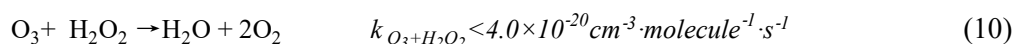


Fig. 9. Effect of  $\text{H}_2\text{O}$  on NO oxidation efficiency of  $\text{O}_3$  oxidation. Conditions:  $[\text{NO}]_{\text{in}} = 500 \text{ ppm}$ ,  $\text{O}_2$  content = 3 vol.%, flue gas temperature =  $150 \text{ }^\circ\text{C}$ , flue gas flow rate =  $1.0 \text{ L}\cdot\text{min}^{-1}$ .

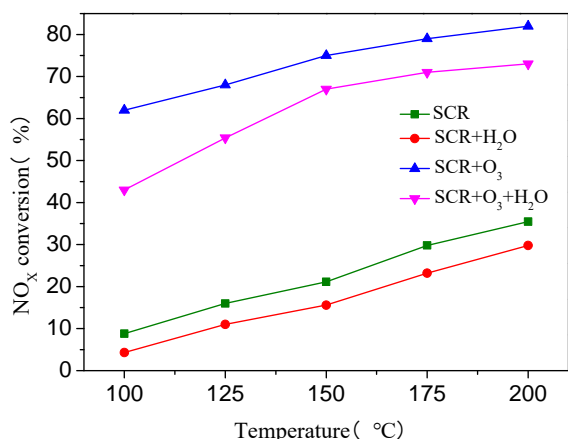


Fig. 10. Effect of H<sub>2</sub>O on NO<sub>x</sub> removal efficiency in O<sub>3</sub>-NH<sub>3</sub>-SCR system. Conditions: [NO]<sub>in</sub> = [NH<sub>3</sub>] = 500 ppm, O<sub>3</sub> concentration = 250 ppm, O<sub>2</sub> content = 3 vol.%, H<sub>2</sub>O content = 6 vol.%, flue gas temperature = 150 °C, flue gas flow rate = 1.0 L·min<sup>-1</sup>, and GHSV = 25000 h<sup>-1</sup>.

Fig. 10 shows the effect of the presence of H<sub>2</sub>O in the flue gas on the degradation efficiency of the O<sub>3</sub>-NH<sub>3</sub>-SCR process and the SCR process. At the temperature of 150 °C, the NO<sub>x</sub> removal efficiency with 0 vol.% and 6 vol.% H<sub>2</sub>O in the SCR process was 21.15%, 15.6%, respectively. The temperature was in the range of 100 °C to 200 °C, and NO<sub>x</sub> removal efficiency in the flue gas with 6 vol.% H<sub>2</sub>O was less than that with 0 vol.% H<sub>2</sub>O. This result can be probably explained by the competitive adsorption of H<sub>2</sub>O with NO, NH<sub>3</sub> and other reactive molecules on the catalyst surface. Another reason was that the hydroxylation of H<sub>2</sub>O occurred on the catalyst surface, resulting in a decrease in the redox capacity of the catalyst. And hydroxylation reaction was generally non-renewable for low temperature NH<sub>3</sub>-SCR process [33, 34]. However, compared with SCR, O<sub>3</sub>-NH<sub>3</sub>-SCR process had a significantly improved NO<sub>x</sub> removal efficiency at the temperature of 150 °C, and the NO<sub>x</sub> removal efficiency with the presence of H<sub>2</sub>O of 0 vol.% and 6 vol.% were 75.0% and 67.0%, respectively. Experiment showed that the presence of water vapor reduced the NO<sub>x</sub> removal efficiency in O<sub>3</sub>-NH<sub>3</sub>-SCR system. The reason for this phenomenon was that water vapor affected the process of NO conversion to NO<sub>2</sub> and had a toxic effect on the catalyst surface. Therefore, the addition of ozone only enhanced the NO<sub>x</sub> degradation effect, but could not improve the water resistance of the catalyst.

### 3.5 Effect of SO<sub>2</sub> on the NO<sub>x</sub> removal

Fig. 11 shows the effect of the presence of SO<sub>2</sub> in the simulated flue gas on the oxidation efficiency of NO. The concentration of O<sub>3</sub> in the simulated flue gas was 250 ppm, and the concentration of SO<sub>2</sub> was 200 ppm. The composition of outlet exhaust gas was determined by FTIR. When SO<sub>2</sub> was contained in the simulated flue gas, no SO<sub>3</sub> was detected in all cases, which might be attributed to the oxidation rate of SO<sub>2</sub> was very low and the concentration of SO<sub>3</sub> produced was under the detection limit [35]. According to the formula 11, the reaction of O<sub>3</sub> and SO<sub>2</sub> was difficult to carry out. Therefore, the presence of SO<sub>2</sub> under this condition hardly affected the oxidation efficiency of NO by ozone oxidation.



The effect of SO<sub>2</sub> in simulated flue gas on the NO<sub>x</sub> removal efficiency in the O<sub>3</sub>-NH<sub>3</sub>-SCR and SCR process is shown in Fig. 12. In SCR and O<sub>3</sub>-NH<sub>3</sub>-SCR systems, the catalyst still maintained a stable NO<sub>x</sub> removal efficiency after 60 min on stream. However, with the addition of SO<sub>2</sub>, the NO<sub>x</sub> removal efficiency of the SCR system decreased from 21.4% to 9.9% after 120 minutes. Similarly, the NO<sub>x</sub> removal efficiency of the O<sub>3</sub>-NH<sub>3</sub>-SCR system reduced from 75.8% to 55.9%. And the O<sub>3</sub>-NH<sub>3</sub>-SCR system exhibited superior SO<sub>2</sub> resistance than SCR system. The reason of decrease in NO<sub>x</sub> removal efficiency might be described to the formation of sulfate which could cover the surface active center of catalyst and result in the deactivate of catalyst [36]. Therefore, when SO<sub>2</sub> was contained in the flue gas, O<sub>3</sub>-NH<sub>3</sub>-SCR process can significantly

improve the NO<sub>x</sub> degradation efficiency compared with the SCR process, but the inhibition effect of the SO<sub>2</sub> on the catalyst still existed.

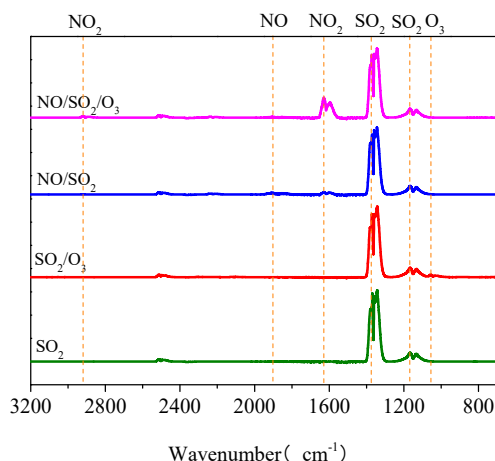


Fig. 11. Effect of SO<sub>2</sub> on NO oxidation efficiency.

Conditions: [NO]<sub>in</sub> = 500 ppm, O<sub>3</sub> concentration = 250 ppm, O<sub>2</sub> content = 3 vol.%, SO<sub>2</sub> concentration = 250 ppm, flue gas temperature = 150 °C, flue gas flow rate = 1.0 L·min<sup>-1</sup>.

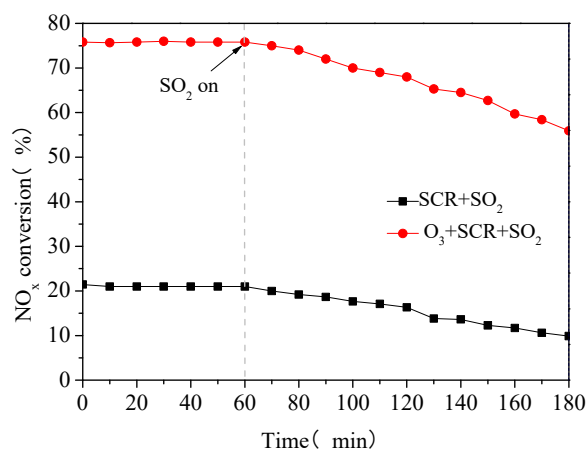


Fig. 12. Effect of SO<sub>2</sub> on NO<sub>x</sub> removal efficiency in O<sub>3</sub>-NH<sub>3</sub>-SCR system.

Conditions: [NO]<sub>in</sub> = [NH<sub>3</sub>]<sub>in</sub> = 500 ppm, O<sub>3</sub> concentration = 250 ppm, O<sub>2</sub> content = 3 vol.%, SO<sub>2</sub> concentration = 250 ppm, flue gas temperature = 150 °C, flue gas flow rate = 1.0 L·min<sup>-1</sup>, and GHSV = 25000 h<sup>-1</sup>.

#### 4. Conclusion

In this study, the key influencing factors on the oxidation of NO by ozone were studied, including O<sub>3</sub>/NO molar ratio, residence time and reaction temperature. Reaction temperature of the flue gas was the main factor affecting the decomposition of O<sub>3</sub>. The decomposition rate of O<sub>3</sub> was slow at low temperature and increased significantly when temperature exceeded 150 °C. In addition, when the O<sub>3</sub>/NO molar ratio was below 0.8, the oxidation product of NO was only NO<sub>2</sub>.

The effect of O<sub>3</sub> injection position and other components, such as O<sub>3</sub>/NO molar ratio, H<sub>2</sub>O and SO<sub>2</sub>, on the NO<sub>x</sub> removal efficiency of O<sub>3</sub> assisted SCR system were also studied. The results indicated that the O<sub>3</sub> assisted SCR process obviously improved the removal efficiency of NO<sub>x</sub> in the standard SCR process at the temperature below 250 °C. In addition, the O<sub>3</sub>-NH<sub>3</sub>-SCR system had better NO<sub>x</sub> removal effect than the NH<sub>3</sub>-O<sub>3</sub>-SCR system. SO<sub>2</sub> had almost no effect on NO oxidation efficiency, while H<sub>2</sub>O had a certain inhibitory effect on NO oxidation efficiency. The NO<sub>x</sub> removal of O<sub>3</sub>-NH<sub>3</sub>-SCR system was also inhibited by H<sub>2</sub>O and SO<sub>2</sub> at low temperature, but the NO<sub>x</sub> removal of O<sub>3</sub>-NH<sub>3</sub>-SCR process was still significantly better than the SCR process.

## References

- [1] Miyazaki K., Decadal changes in global surface NO<sub>x</sub> emissions from multi-constituent satellite data assimilation, *Atmos. Chem. Phys.*, Vol. 17, pp. 807–837, 2017.
- [2] Boningari T., and Smirniotis P.G., Impact of nitrogen oxides on the environment and human health: Mn-based materials for the NO<sub>x</sub> abatement, *Curr. Opin. Chem. Eng.*, Vol. 13, pp. 133–141, 2016.
- [3] Koebel M., Elsener M., and Kleemann M., Urea-SCR: a promising technique to reduce NO<sub>x</sub> emissions from automotive diesel engines, *Catal. Today*, Vol. 59, pp. 335–345, 2000.
- [4] Koebel M., Madia G., and Elsener M., Selective catalytic reduction of NO and NO<sub>2</sub> at low temperatures, *Catal. Today*, Vol. 73, pp. 239–247, 2002.
- [5] Colombo M., Nova I., and Tronconi E., Detailed kinetic modeling of the NH<sub>3</sub>–NO/NO<sub>2</sub> SCR reactions over a commercial Cu-zeolite catalyst for diesel exhausts after treatment, *Catal. Today*, Vol. 197 (1), pp. 243–255, 2012.
- [6] Xin Y., Li Q., and Zhang Z., Zeolitic materials for DeNO<sub>x</sub> selective catalytic reduction, *ChemCatChem*, Vol. 10, pp. 29–41, 2018.
- [7] Li J., Chang H. and Hao J., Low-temperature selective catalytic reduction of NO<sub>x</sub> with NH<sub>3</sub> over metal oxide and zeolite catalysts—A review, *Catal. Today*, Vol. 175, pp. 147–156, 2011.
- [8] Tronconi E., Nova I. and Ciardelli C., Redox features in the catalytic mechanism of the “standard” and “fast” NH<sub>3</sub>–SCR of NO<sub>x</sub> over a V-based catalyst investigated by dynamic methods, *J. Catal.*, Vol. 245 (1), pp. 1–10, 2007.
- [9] Grossale A., Nova I., and Tronconi E., Ammonia blocking of the “fast SCR” reactivity over a commercial Fe-zeolite catalyst for diesel exhaust after treatment, *J. Catal.*, Vol. 265 (2), pp. 141–147, 2009.
- [10] Iwasaki M., and Shinjoh H., A comparative study of “standard”, “fast and NO<sub>2</sub> SCR reactions over Fe/zeolite catalyst, *Appl. Catal. A: Gen.*, Vol (1–2). 390, pp. 71–77, 2010.
- [11] Salazar M., Hoffmann S. and Singer V., Hybrid catalysts for the selective catalytic reduction (SCR) of NO by NH<sub>3</sub>. On the role of fast SCR in the reaction network, *Appl. Catal. B: Environ.*, Vol.199, pp. 433–438, 2016.
- [12] Koebel M., Elsener M. and Madia G., Reaction pathways in the selective catalytic reduction process with NO and NO<sub>2</sub> at low temperatures, *Ind. Eng. Chem. Res.*, Vol. 40 (1), pp. 52–59, 2001.
- [13] Gao F., Kollár M. and Kukkadapu R. K., Fe/SSZ–13 as an NH<sub>3</sub>–SCR catalyst: A reaction kinetics and FTIR/Mössbauer spectroscopic study, *Appl. Catal. B: Environ.*, Vol. 164, pp. 407–419, 2015.
- [14] Millo F., Ragaini M., Fino D. and Miceli P., Application of a global kinetic model on an SCR coated on Filter (SCR–F) catalyst for automotive applications, *Fuel*, Vol. 198, pp. 183–192, 2017.
- [15] Oskooei A. B., Koohsorkhi J., and Mehrpooya M., Simulation of plasma-assisted catalytic reduction of NO<sub>x</sub>, CO and HC from diesel engine exhaust with COMSOL, *Chem. Eng. Sci.*, Vol. 197, pp. 135–149, 2019.
- [16] Chmielewski A. G. i, Ostapczuk A., Zimek Z., Licki J. and Kubica K., Reduction of VOCs in flue gas from coal combustion by electron beam treatment, *Radiation Phys. Chem.*, Vol. 63 (3–6), pp. 653–655, 2002.
- [17] Wu Z., Study of a photocatalytic oxidation and wet absorption combined process for removal of nitrogen oxides, *Chem. Eng. J.*, Vol. 144, pp. 221–226, 2008.
- [18] Wu Q., Sun C., Wang H., Wang T., Wang Y. and Wu Z., The role and mechanism of triethanolamine in simultaneous absorption of NO<sub>x</sub> and SO<sub>2</sub> by magnesia slurry combined with ozone gas-phase oxidation, *Chem. Eng. J.*, Vol. 341, pp. 157–163, 2018.
- [19] S. Byoun, D. N. Shin, I. S. Moon and Y. Byun, Quick vaporization of sprayed sodium hypochlorite (NaClO<sub>(aq)</sub>) for simultaneous removal of nitrogen oxides (NO<sub>x</sub>), sulfur dioxide (SO<sub>2</sub>), and mercury (Hg<sup>0</sup>), *J. Air Waste Manag. Assoc.*, Vol. 69 (7), pp. 857–866, 2019.
- [20] Yang B., Ma S., Cui R., Sun S., Wang J. and Li S., Simultaneous removal of NO<sub>x</sub> and SO<sub>2</sub> with H<sub>2</sub>O<sub>2</sub> catalyzed by alkali/magnetism-modified fly ash: High efficiency, low cost and catalytic mechanism, *Chem. Eng. J.*, Vol. 359, pp. 233–243, 2019.
- [21] Pan W., Zhang X. and Guo R., A thermodynamic study of simultaneous removal of SO<sub>2</sub> and NO by a KMnO<sub>4</sub>/ammonia solution, *Energy Sources, Part A: Recovery, Utilization, and Environmental Effects*, Vol. 37 (7), pp. 721–726, 2015.
- [22] Stamate E., Chen W. and Jørgense L., IR and UV gas absorption measurements during NO<sub>x</sub> reduction on an industrial natural gas fired power plant, *Fuel*, Vol. 89 (5), pp. 978–985, 2010.
- [23] Zhang J., Zhang R. and Che X., Simultaneous removal of NO and SO<sub>2</sub> from flue gas by ozone oxidation and NaOH absorption, *Ind. Eng. Chem. Res.*, Vol. 53 (15), pp. 6450–6456, 2014.
- [24] Yao S., Wu Z., Han J. and Tang X., Study of ozone generation in an atmospheric dielectric barrier discharge reactor, *J. Electrostat.*, Vol. 75, pp. 35–42, 2015.
- [25] Luo S., Zhou W., Xie A., and F. Wu, Effect of MnO<sub>2</sub> polymorphs structure on the selective catalytic reduction of NO<sub>x</sub> with NH<sub>3</sub> over TiO<sub>2</sub>–Palygorskite, *Chem. Eng. J.*, Vol. 286, pp. 291–299, 2016.
- [26] Blanco J., Avila P. and Suárez S., CuO/NiO monolithic catalysts for NO<sub>x</sub> removal from nitric acid plant flue gas, *Chem. Eng. J.*, Vol. 97, pp. 1–9, 2004.

- [27] Boningari T., Somogyvari A., and Smirniotis P. G., Ce-based catalysts for the selective catalytic reduction of NO<sub>x</sub> in the presence of excess oxygen and simulated diesel engine exhaust conditions, *Ind. Eng. Chem. Res.*, Vol. 56 (19), pp. 5483–5494, 2017.
- [28] Shan W., Liu F., He H., Shi X., and Zhang C., An environmentally-benign CeO<sub>2</sub>-TiO<sub>2</sub> catalyst for the selective catalytic reduction of NO<sub>x</sub> with NH<sub>3</sub> in simulated diesel exhaust, *Catal. Today*, Vol. 184, pp. 160–165, 2012.
- [29] Gao X., Du X. S., and Cui L., A Ce-Cu-Ti oxide catalyst for the selective catalytic reduction of NO with NH<sub>3</sub>, *Catal. Commun.*, Vol. 12 (4), pp. 255–258, 2010.
- [30] Li X., and Li Y., Selective Catalytic Reduction of NO with NH<sub>3</sub> over Ce-Mo-Ox Catalyst. *Catal. Lett.*, Vol. 144, pp. 165–171, 2014.
- [31] De Pena R. G., Olszyna K., and Heickle J., Kinetics of particle growth. I. Ammonium nitrate from the ammonia-ozone reaction, *J. Phys. Chem.*, Vol. 77 (4), pp. 438–443, 1973.
- [32] Wallington T. J., Jucks K. W., and Tyndal G. S. I, Upper limits for the gas-phase reaction of H<sub>2</sub>O<sub>2</sub> with O<sub>3</sub> and NO. Atmospheric implications, *Int. J. Chem. Kinetics*, Vol. 30, pp. 707–709, 1998.
- [33] Xiao X.Xiong S., Shi Y., Shan W., and Yang S., Effect of H<sub>2</sub>O and SO<sub>2</sub> on the selective catalytic reduction of NO with NH<sub>3</sub> over Ce/TiO<sub>2</sub> catalyst: Mechanism and kinetic study, *J. Phys. Chem. C*, Vol. 120 (2), pp. 1066–1076, 2016.
- [34] Tong H., Dai J., He Y., and Tong Z., The effects of H<sub>2</sub>O and SO<sub>2</sub> on the behaviour of CuSO<sub>4</sub>-CeO<sub>2</sub>/TS for low temperature catalytic reduction of NO with NH<sub>3</sub>, *Environ. Technol.*, Vol. 32 (8), pp. 891–900, 2011.
- [35] Li B., Zhao B., and Lu J., Numerical study of the simultaneous oxidation of NO and SO<sub>2</sub> by ozone, *Int. J. Environ. Res. Public Health*, Vol. 12 (2), pp. 1595–1611, 2015.
- [36] Liu F., and He H., Selective catalytic reduction of NO with NH<sub>3</sub> over manganese substituted iron titanate catalyst: Reaction mechanism and H<sub>2</sub>O/SO<sub>2</sub> inhibition mechanism study, *Catal. Today*, Vol. 153 (3–4), pp. 70–76, 2010.